Electrical Response of Polypyrrole Films Doped with Dodecylbenzene Sulfonic Acid to Acetone Vapor

M. Campos

UNIP- Universidade Paulista, Grupo de Pesquisa "Ciência dos Materiais", CEP 14025-270 Ribeirão Preto, SP, Brazil

Received 20 August 2010; accepted 2 December 2010
DOI 10.1002/app.33959
Published online 23 March 2011 in Wiley Online Library (wileyonlinelibrary.com).

ABSTRACT: Measurements of current-voltage curves at room temperature, in nitrogen and nitrogen-acetone atmospheres have clearly demonstrated the rectifying behavior of the Al/PPy-DBSA/Au structure. For this structure, the values of 0.82 eV and 2.31, for the barrier height and ideality factor, respectively, have been obtained in nitrogen atmosphere, while at concentration of 120 ppm of acetone, the corresponding values were 0.74 eV and 2.07. The barrier height value obtained from I–V characteristic is lower than the barrier height value obtained from C-V measurements. The discrepancy can be due to the existence of an interfacial oxide layer between the semiconductor and Schottky contact metal. The density distribution curves of the interface states vary in the range ($0.55–E_V$) to ($0.84–E_V$) for pure nitrogen, and ($0.45–E_V$) to ($0.60–E_V$) in atmosphere with acetone. The interface state density has an exponential rise with bias from the midgap towards the top of the valence band of the PPy-DBSA. © 2011 Wiley Periodicals, Inc. J Appl Polym Sci 121: 2518–2525, 2011

Key words: conducting polymer; acetone; electrical current; capacitance

INTRODUCTION

Conducting polymers have been widely investigated with the objective of improving their processability, and their physical and chemical properties. Many promising applications have emerged from the application of conducting polymers. One such application is in gas sensor technologies, where measurement of changes in the conducting polymer electrical properties, when exposed to an analyte vapor, can form the basis of the sensor system. The sensors based on conductive polymer can be operated at room temperature. They are light, noncorrosive, and can be easily prepared. Polypyrrole (PPy) is one of the most interesting, among many conductive polymers known, due to its relatively high environmental stability[1] and the ease of synthesizing and doping with various dopants.[2] The versatility of this polymer is determined by a number of properties: redox activity,[3] ability to form nanowires,[4] ion exchange and ion discrimination capacities,[5] electrochromic effect, depending on electrochemical polymerization conditions, and charge/discharge processes.[6] Also, it presents strong absorptive properties towards gases,[7] proteins,[8] DNA,[9] catalytic activity,[10] corrosion protection properties,[11] etc.

The effect of gases on the electrical conductivity of polypyrrole has been known since 1996.[12] After first grown electrochemically[13] polypyrrole has been used in gas sensors that measure the change of the electrical resistivity in the presence of different gases.[14] Gases interacting with conducting polymers can be divided in two categories: gases which react chemically with it and gases that are adsorbed by it. Chemical reactions lead to changes in the conducting polymer doping level and alter the electrical resistance and optical absorption. Adsorbed gases change the depletion region and thus modulate the electrical conductivity of the junction.[15–18] Electron accepting gases, with an electron affinity bigger than that of the conducting polymer are able to oxidize the conducting polymer. Electron donating gases reduce and therefore dedope conducting polymers, which leads to an increase in electrical resistance.[19] Weak physical interactions of nonreactive volatile organic compounds, like acetone with the polymer, may lead to modification of the electrical resistance of the conducting polymer. Acetone is a commonly used chemical reagent in industry, to dissolve plastics, dehydrate tissues, purify paraffin, and for pharmaceutical applications. It is easy to evaporate at room temperature. People exposed to such vapor may develop headaches, fatigue and even narcosis, when the concentration of acetone in air is higher than 10,000 ppm. Additionally, the medical reports show that acetone is one of the products exhaled by

Correspondence to: M. Campos (campos@unip.br).
Contract grant sponsor: Vice-Reitoria de Pesquisa e Pós-Graduação da Universidade Paulista (UNIP), Brazil.

diabetic patients who have higher acetone concentrations in their blood and spittle than healthy people.[20,21] Hence, detecting and measuring acetone concentrations in the workplace or in the human body are necessary for our safety and health.

The aim of this study is to obtain some properties of Al/PPy-DBSA/Au structure measured in atmospheres of nitrogen with different concentrations of acetone. For that, electrical current-voltage (*I–V*) and capacitance-voltage (*C–V*) characteristics, as well as interface state density distribution properties of interface states, were measured. These measurements were done in the dark, at room temperature (25°C) and with relative humidity of 50% RH.[22]

EXPERIMENTAL

Materials and sample preparation

Pyrrole monomer (AR grade, Fluka) was dried with calcium hydride (CaH_2), for 24 h, and was purified by distillation under reduced pressure. Ammonium persulfate (APS) (AR grade, Sigma-Aldrich) as an oxidant and dodecylbenzene sulfonic acid (DBSA) (AR grade, Sigma-Aldrich) were used as dopant without further purification. Soluble polypyrrole was synthesized by chemical oxidation according to the method reported earlier.[23,24] DBSA (0.15 mol, 48 g) and pyrrole (0.40 mol, 26.6 g) were added to distilled deionized water (250 mL) with vigorous stirring. The reaction vessel was kept in an ice bath. The oxidant (0.06 mol), dissolved in 75 mL of distilled water, was added dropwise over a period of about 60 min into the monomer solution, with polymerization purpose. PPy started to precipitate immediately. The reaction was carried out for two days, stirring during the first 4 h. Polypyrrole was formed as powder, which was filtered and sequentially washed with methanol and distilled water and dried in a vacuum at room temperature for two days. To prepare the solutions, 1 g of PPy was dissolved in 40 mL of *m*-cresol with 2 g of DBSA added. The solution was filtered and poured onto a glass plate and the solvent was slowly evaporated. The resulting film was peeled off from the glass plate and washed with methanol. Then the free-standing film was dried under dynamic vacuum at 50°C for one day. The quantities used for monomer, oxidant, and dopant were chosen following Lee recommendations.[25,26]

The thickness of the prepared films was of about 10–25 μm. Circular electrodes of about 0.38 cm^2 were vacuum (10^{-5} Torr) deposited on each face of the samples. The electrodes were aluminum on one side, and gold on the other face of the samples.

Gas test measurements were carried out at constant temperature (room temperature) by recording the dynamic changes in electrical current caused by the exposure to different concentrations (10–200 ppm) of acetone in dry nitrogen. These concentrations are below the limit imposed on the breath analyzer.[27]

Gas chamber

A chamber was constructed to allow an efficient gas mixing, to ensure vapor homogeneity at the sensor gas interface. The gas chamber consists of a closed stainless steel cylinder with capacity of 1.8×10^3 cm^3, attached to a nitrogen flow controller and with connections allowing measurements of electrical current-voltage (two probes), capacitance-voltage and capacitance-frequency characteristics. The appropriate amount of acetone to produce the predetermined concentrations was injected into the reservoir using a micro-syringe via a septum fitted in the chamber. The volume of acetone vapor in the container at 25°C was varied from 10% of LEL (lower explosive limit, 0.25 vol %) to 25% of UEL (upper explosive limit, 30 vol %).[28]

The acetone evaporated quickly in the chamber (<30 s). All the measurements were made after the sample was about 10 min in the acetone atmosphere. Few minutes exposure to vapor was sufficient to stabilize the electrical conductivity, the 10-min exposure was performed to ensure equilibrium.

A flux of nitrogen of about 2 L/min during about 4 h was used to clean the system and to allow the polypyrrole recover its baseline electrical resistance values. The measurements were done in the dark, at room temperature (25°C) and relative humidity of 50%. To maintain RH constant, dry N_2 was flown into the system, passing through a water container or a desiccator to increase or decrease RH in the chamber.

Instruments

The electrical current-voltage characteristics (*I–V*) at room temperature (25°C) were recorded with the help of a Keithley model 6517A electrometer and a Keithley model 2400 source meter. The sample temperature was always monitored by using a copper-constantan thermocouple, close to the sample, and measured with a dmm/scanner Keithley model 199. The capacitance-voltage measurements (*C–V*) were performed at room temperature, using a Solartron 1255 frequency response analyzer coupled with a Solartron 1286 electrochemical interface. All measuring instruments were connected to a computing system to collect the data and calculate the desired properties.

RESULTS AND DISCUSSION

Acetone sensing

Acetone test measurements were carried out at room temperature by recording the changes in electrical current caused by the exposure to different concentrations of acetone vapors in dry nitrogen. The dynamics of the process is fast, as indicated by the response time of about 20 s. A typical response curve as a function of time, for different acetone concentrations, is showed in Figure 1, for applied voltage of 0.5 V, 50% RH and sample thickness of 12 μm. These results show a decrease of the current density as the acetone concentration increases.

Electrical current-voltage characteristics

Some years ago, it was proposed that the nonlinearity of the *I–V* characteristics of the polymer/metal junction could be due to space-charge limited conduction (SCLC),[29] Poole-Frenkel emission[30] or thermionic emission.

A system will follow the SCLC mechanism if the plot of log (*I*) versus log (*V*) is linear. Also, if we have a Poole-Frenkel emission mechanism, log (*J*) versus $(E)^{1/2}$ should be linear, *J* being the electrical current density and *E* the applied electrical field. For our samples linearity was not observed in neither case. These results suggest that the thermionic emission theory can be applied.

According to the thermionic emission theory without tunneling and diffusion, the forward *I–V* characteristics of Schottky barrier diodes can be expressed as[31]

$$I = I_0\{\exp[qV/(nkT)] - 1\} \quad (1)$$

where the saturation current is given by

$$I_0 = AA^* T^2 \exp[-q\phi/(kT)] \quad (2)$$

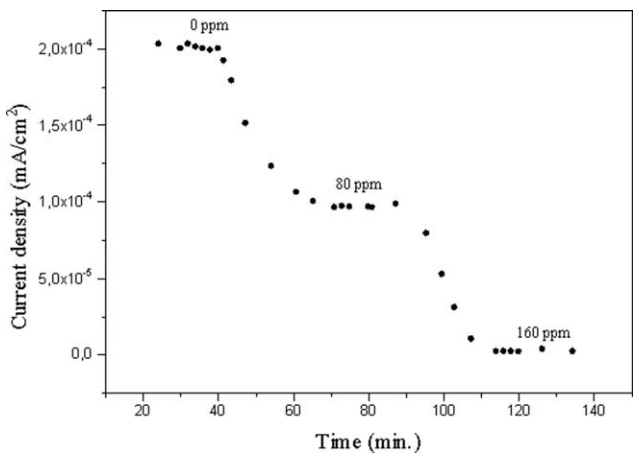

Figure 1 Electrical current density as a function of time for acetone concentrations of 0 ppm, 80 ppm, and 160 ppm at room temperature, 50% RH and applied voltage of 0.5 V.

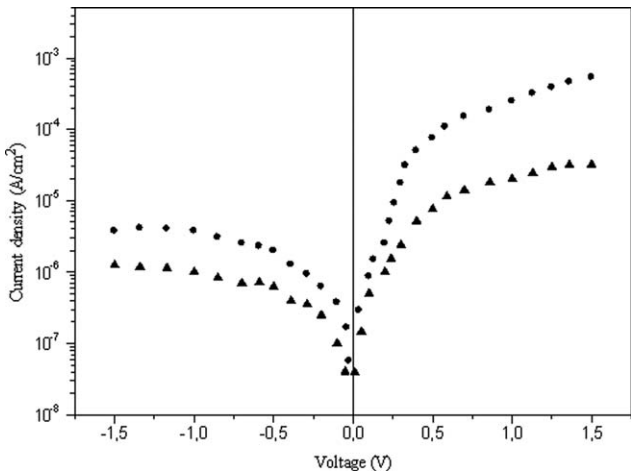

Figure 2 Electrical current density as a function of applied voltage for the structure Al/PPy-DBSA/Au in atmosphere of pure nitrogen (■) and 70 ppm of acetone (▲), at room temperature and 50% RH.

φ is the effective barrier height at zero bias, A^* is the Richardson constant and equal to 120 A/cm^2 K^2 for free electron, *q* is the electron charge, *V* is the forward bias voltage, *A* is the effective diode area, *k* is the Boltzmann's constant, T is the temperature in Kelvin, n is the ideality factor. The ideality factor was determined from the slope of the linear region of the forward bias ln(*I*)-*V* characteristics through the relation:

$$n = q/[(kT)dV/d(\ln I)] \quad (3)$$

Also, from eq. (1), the voltage dependent ideality factor $n(V)$ can be written as

$$n(V) = qV/[kT \ln (I/I_0)] \quad (4)$$

Ideality factor higher than unity shows the presence of nonideal *I–V* behavior, and can be attributed to many possibilities: presence of the interfacial layer,[32] barrier inhomogeneities,[33] bias dependence of the barrier height, series resistance, tunneling currents,[34] image force lowering of the Schottky barrier,[35] generation-recombination currents within the space-charge region.[36] Auger profiling analysis of Al/PPy interfaces showed the presence of an insulating between the metal and the polymer,[37] so we are going to assume that we have a native oxide layer (probably Al_2O_3) between Al and PPy, that was growing during Al deposition.[38]

The barrier height can be obtained from eq. (2):

$$q\phi = kT \ln [A A^* T^2/(I_0)] \quad (5)$$

Figure 2 shows the electrical current density-voltage characteristics of Al/PPy-DBSA/Au diode measured in nitrogen and acetone concentration of 70 ppm, at room temperature, 50% RH and sample

TABLE I
Values Obtained for the Saturation Current (J_0), Amplification Factor, Factor of Ideality (n) and Barrier Height (φ) at Room Temperature and 50% RH as a Function of Acetone Concentration

Concentration (ppm)	J_0 (10^{-6} A/cm^2)	Amplification	n	φ (eV)
40	9.39	1576	1.85	0.80
80	7.84	1344	1.98	0.78
120	7.03	1187	2.07	0.74
160	5.45	926	2.12	0.71

thickness of 14 μm. As can be seen from the figure, the presence of acetone decreases the electrical current density.

Measurements of XPS and FT-IR[39] showed that this effect is probably due to the increase of nitrogen imine (=N-) in PPy due to the interaction with acetone. Also, it was possible to see that at about 0.5 V, the electrical current density starts to saturate. This means that the externally applied electrical voltage differs from V, due to the fact that the layer causes a voltage drop across the interface.

Varying the acetone concentration and using eqs. (4) and (5) it was possible to calculate the Schottky parameters at room temperature, what is showed in Table I.

From this results, an increase of the ideality factor and a decrease of the barrier height as a function of acetone concentration can be observed. In nitrogen atmosphere the values obtained for the ideality factor and the barrier height were 2.31 and 0.82 eV, respectively.

These results indicate that the electrical current might occur due to mechanisms like tunneling through the barrier, or image force lowering of the barrier height. The effective barrier height due to tunneling is given by[31]

$$\Delta\Phi = (1.5\ E_{00})^{2/3}(V_{\mathrm{bd}})^{1/3} \tag{6}$$

with

$$E_{00} = (h/4\pi)\ (N_d/m^*\in)^{1/2} \tag{7}$$

where N_d is the doping concentration, m^* the effective mass of the carrier, $\in$ the permittivity and V_{bd} the voltage corresponding to band bending. However, according to eq. (6), Δφ should be independent of temperature, although the measured values do depend on temperature. Using typical values in eq. (6) the value obtained for Δφ is too high, so image force alone cannot explain the results. So, tunneling and image force are not good models to explain the results.

Supposing that we have thick interfacial layer,[40] the bias dependence on the voltage drop V_d can be expressed as[41]

$$V_d = (1 - 1/n)V \tag{8}$$

Taken into account the effect of series resistance (R_S), eq. (8) can be written as

$$V_d = (1 - 1/n)(V - \mathrm{IR}_S) \tag{9}$$

The voltage drop across depletion layer (V_{DL}) will be

$$V_{\mathrm{DL}} = V - V_d \tag{10}$$

Figure 3 shows ln (I) versus V for a concentration of acetone of 50 ppm, using the values obtained for V_d and V_{DL}. It is possible to see from the figure that there is effect of interface layer on the parameters of the diode.

The series resistance R_S, as well as other Schottky diode parameters, such as ideality factor n and barrier height φ, were also determined using the Cheung's functions.[42] Equation 1 can be rewritten as:

$$I = I_0\{\exp[(q/nkT)(V - \mathrm{IR}_S)] - 1\} \tag{11}$$

From eq. (11) we get:

$$V = \mathrm{IR}_S + n\phi + (nkT/q)\ \ln\ (I/AA^*T^2) \tag{12}$$

$$dV/d[(\ln\ (I)] = (nkT/q) + \mathrm{IR}_S \tag{13}$$

With the help of

$$H(I) = V - (nkT/q)\ \ln\ (I/AA^*T^2) \tag{14}$$

we can write

$$H(I) = I\ R_S + n\phi \tag{15}$$

For the downward curvature region in the forward bias I–V characteristics, eqs. (13) and (15) correspond

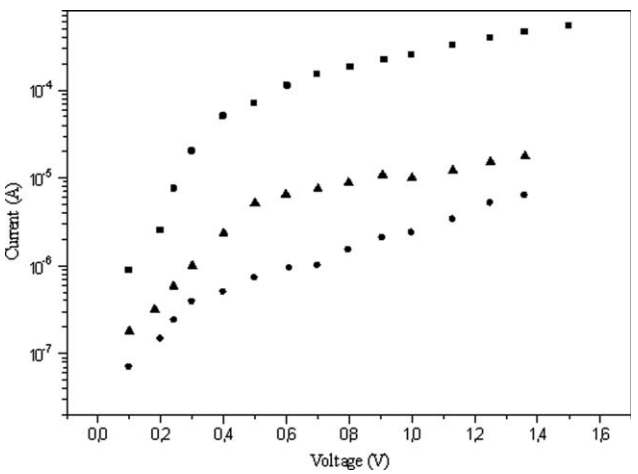

Figure 3 Variations of forward current of the diode in atmosphere of 50 ppm of acetone with the values of V (■), V_d (●), and V_{DL}(▲) at room temperature and 50% RH.

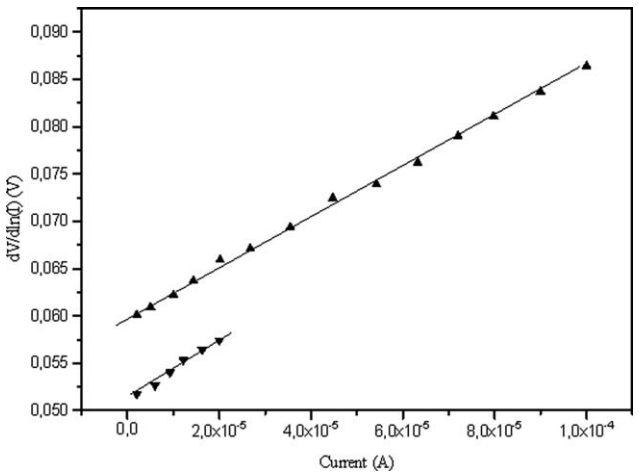

Figure 4 Plot of dV/d(lnI) as a function of electrical current for the diode in atmosphere of nitrogen (▲) and acetone concentration of 120 ppm (▼) at room temperature and 50% RH.

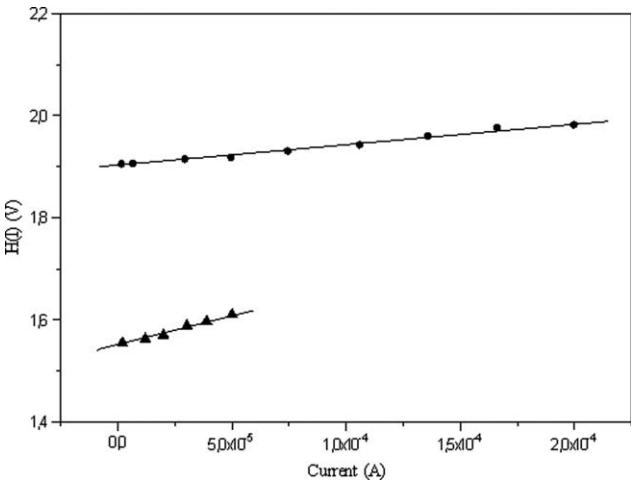

Figure 5 Plot of H (I) as a function of electrical current for atmosphere of nitrogen (■) and acetone in the concentration of 120 ppm (●) at room temperature and 50% RH.

to straight lines, as is showed in Figures 4 and 5. The acetone concentration in both experiments was 120 ppm.

The values of n and φ obtained from the vertical axis intercepts of dV/d[ln(I)] and H(I) versus I curves and the values of R_S from their slopes, are showed in Table II.

As can be seen from Tables I and II, there is a significant difference between the values of n and φ obtained from the downward curvature regions of forward bias I–V plots, and from the linear regions of the same characteristics. This can be attributed to the existence of series resistance and bias dependence of φ in agreement to the voltage drop across the interfacial layer and change of the interface states with bias, in this concave region of the I–V plot. In Figure 6 it is possible to see the variation of the internal series resistance as a function of acetone concentration. As can be observed from the figure, the internal resistance increases with the increase of the acetone concentration.

Capacitance-voltage characteristics

Figure 7 shows the experimental C versus V curves of the Al/PPy-DBSA/Au structure in the frequency range from 100 kHz to 600 kHz at room temperature and 50% RH, in atmospheres of pure nitrogen and concentration of acetone of 150 ppm.

These results show that the values of the capacitance raise to a peak value and then decrease, with increasing frequency. This happens probably due to the presence of interface states, inhomogeneity of the barrier and oxide layer at metal/semiconductor interface.

In a Schottky type diode the depletion layer capacitance is written as[43]

$$C^{-2} = 2(V_{\mathrm{bi}} + V)/[A^2 \in_S q N_a] \tag{16}$$

where V_{bi} is the built-in potential, A is the area of diode, ϵ_S is the dielectric constant of semiconductor, N_a is the doping concentration. The built-in potential is determined from the extrapolation of the linear reverse bias C^{-2} versus V plot to the V axis as showed in Figure 8.

The barrier height value can be obtained from C–V measurements from the relation

$$\Phi = V_{\mathrm{bi}} + V_p \tag{17}$$

where V_p is the potential difference between the Fermi level and the top of the valence band in the

TABLE II
Values for Ideality Factor n, Barrier Height φ and Series Resistance R_S in Atmosphere of Nitrogen and 120 ppm of Acetone, at Room Temperature and 50% RH, as Obtained Using eqs. (13) and (15) and the Results of J Versus V

	n		φ (eV)		R_S (Ω)	
	Nitrogen	Acetone	Nitrogen	Acetone	Nitrogen	Acetone
dV/d(lnI)	2.37	1.95	0.80	0.75	247	626
H(I)	2.28	1.98	0.79	0.78	268	673
JxV	2.31	1.99	0.82	0.76	281	618

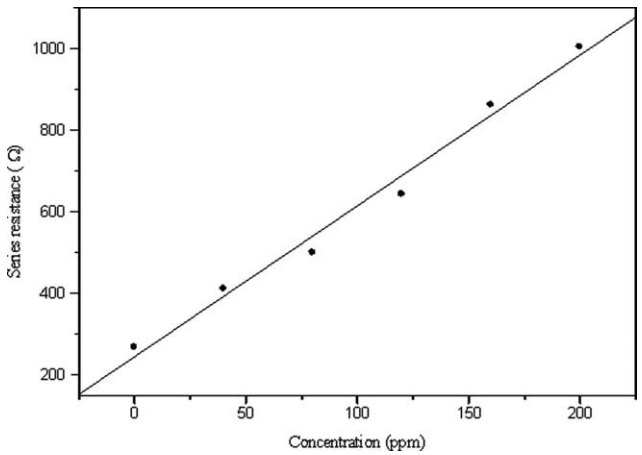

Figure 6 Series resistance as a function of acetone concentration at room temperature and 50% RH.

neutral region of Ppy, and can be obtained by

$$V_p = (kT/q)\ \ln\ (N_v/N_a) \tag{18}$$

where N_v is the effective density of states in the PPy valence band.

As can be observed in Figure 8, the value of the barrier height decreases with increasing frequency, due to a decrease in V_{bi}. Different values for the barrier height were obtained using *I–V* and *C–V* measurements. The difference can be explained by a distribution of barrier height due to the inhomogeneities that occur at metal/PPy interface.

It is believed that the higher value for the ideality factor is due to the voltage drop across an interfacial layer. The density of interface states N_{SS} can be written as[44]

$$N_{SS}(V) = 1/q\{\in_i/\delta[n(V) - 1] - \in_s/W\} \tag{19}$$

ϵ_I and ϵ_S are the permittivity of the interfacial layer and semiconductor, respectively, W is the width of the space charge region and $n(V)$ is the voltage dependent ideality factor. The interfacial insulator layer thickness δ can be obtained from high frequency (1 MHz) *C–V* characteristics using

$$C_i = \in_i \in_0 A/\delta \tag{20}$$

where C_i is the capacitance of the interfacial insulator layer, ϵ_0 is the permittivity of free space A is the area and $\epsilon_i = 8\ \epsilon_0$[44].

From the simple depletion layer theory,[31] the depletion width W can be calculated with

$$W = [2\in_S\ (V_{bi} + V)/(qN_a)]^{1/2} \tag{21}$$

where N_a is calculated using eq. (16) from the slope de $1/C^2$ versus voltage bias.

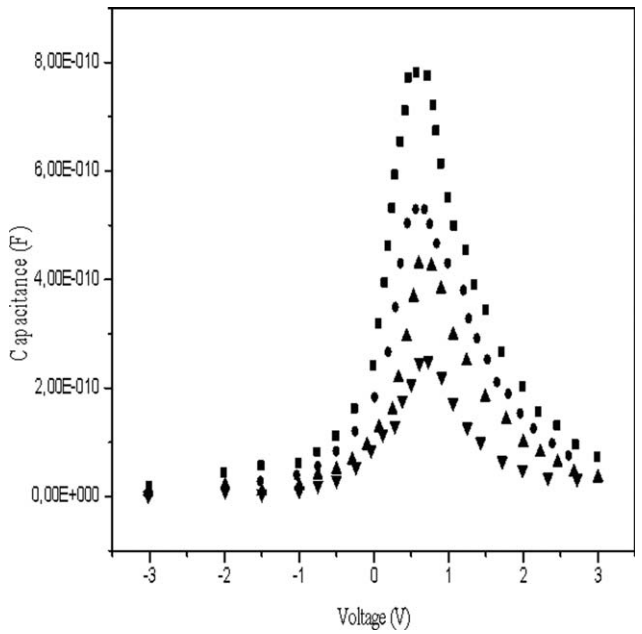

Figure 7 Capacitance as a function of applied voltage at room temperature for frequencies of 100 kHz (■) and 500 kHz (▲) in atmosphere of pure nitrogen, and frequencies of 100 kHz (●) and 500 kHz (▼), for atmosphere with acetone at concentration of 150 ppm.

The different values obtained for the parameters N_a, φ, V_p and W, as a function of frequency in atmosphere of nitrogen and concentration of acetone of 80 ppm, at room temperature and 50% RH are showed in Table III.

As polypyrrole is a *p*-type semiconductor, the energy of interface states E_{SS}, with respect to the top of the valence band is given by

$$E_{SS} - E_V = q(\varphi_{ef} - V) \tag{22}$$

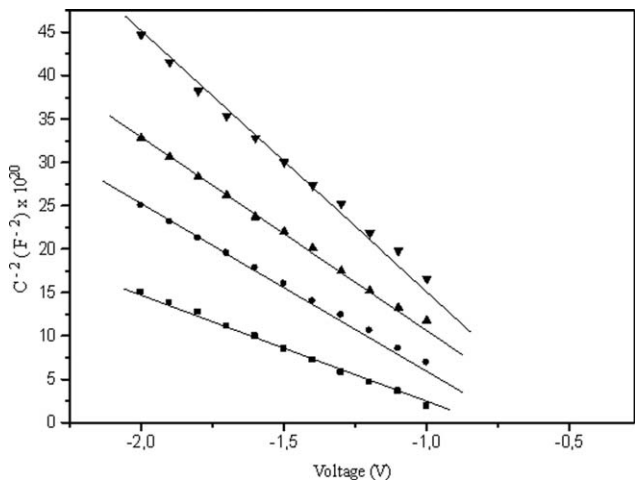

Figure 8 $1/C^2$ as a function of reverse voltage at room temperature in atmosphere of nitrogen and frequencies of 200 kHz (■) and 400 kHz (●), and in atmosphere with 60 ppm of acetone and frequencies of 200 kHz (▲) and 600 kHz (▼).

TABLE III
Parameters of the Schottky Diode Al/PPy-DBSA/Au in Atmosphere of Nitrogen and Acetone Concentration of 80 ppm at Room Temperature and 50% RH for Different Frequencies

	N_a ($\times 10^{14}$ cm^{-3})		φ (eV)		V_P (V)		W ($\times 10^{-4}$ cm)	
f (kHz)	Nitrog.	Acet.	Nitrog.	Acet.	Nitrog.	Acet.	Nitrog.	Acet.
100	5.520	4.406	1.128	0.759	0.373	0.378	1.418	1.530
300	4.314	2.131	0.975	0.713	0.383	0.397	1.497	1.841
500	2.816	1.834	0.811	0.652	0.390	0.401	1.703	1.904
700	2.345	1.687	0.746	0.632	0.395	0.403	1.794	1.958
900	2.232	1.573	0.697	0.626	0.396	0.405	1.783	2.016

Considering the applied voltage dependence of the barrier height, the effective barrier φ_{ef} is given as[45]

$$\Phi_{ef} = \phi + [1 - 1/n(V)](V - IR_S) \quad (23)$$

Using eqs. (20)–(23) the density of interface states N_{SS} as a function of E_{SS}–E_V is shown in Figure 9. The values of the density of interface states are of the order of 10^{14} eV^{-1} cm^{-2}. As we can see from Figure 9, the exponential growth of the interface state density from midgap to the bottom of the valence band is very visible in the range (0.45–E_V) to (0.60–E_V) for atmosphere of acetone (90 ppm) and (0.55–E_V) to (0.84–E_V) for nitrogen.

CONCLUSIONS

The experimental *I–V* and *C–V–f* data of the structure Al/PPy-DBSA/Au were measured in both dry nitrogen and acetone atmospheres, at room temperature and 50% RH. The acetone concentration was varied from 10 to 200 ppm. In both cases the diode has showed rectifying behavior. From the forward (*I–V*) characteristics the ideality factor and barrier height have been obtained as 2.31 and 0.82 eV, in nitrogen atmosphere. For acetone with concentration of 120 ppm we get 2.07 and 0.74 eV, respectively. In both cases, the value of n was greater than unity. This behavior can be ascribed to interfacial layer, interface states, and series resistance. The applied bias voltage drops partially across the oxide layer causing the forward electrical current also to drop, thus producing a deviation from the ideal *I–V* characteristics. The downward curvature at sufficiently large voltages is caused by the effect of series resistance. The experimental results confirmed that in nitrogen or acetone atmospheres the measured capacitance varies with the applied voltage, and frequency and increases with decreasing frequency in depletion and accumulation regions. This happens due to the fact that the distribution of interface states is continuous. The linearity of the C^{-2} versus V characteristics is due to the distribution of the interfacial states density and the donor concentration. The value of the barrier height obtained from *C–V* measurements is higher than the value that was obtained using *I–V* measurements. This discrepancy can be explained by distribution of Schottky barrier height due to inhomogeneities such as nonuniformity of interfacial layer thickness and distributions of the interfacial charges.

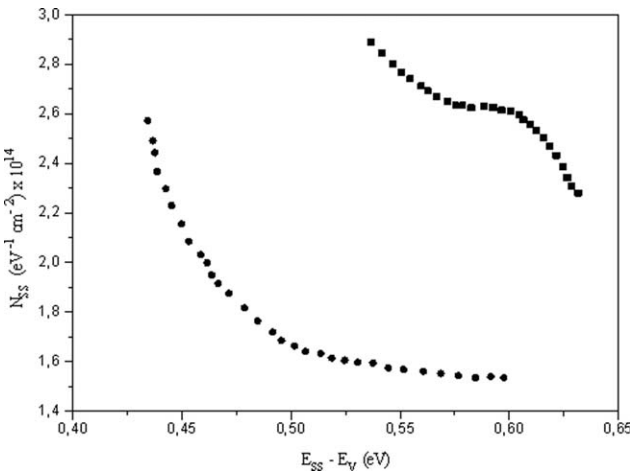

Figure 9 Density of interface states N_{SS} as a function of E_{SS}–E_V for Al/PPy-DBSA/Au Schottky diode as obtained from the *I–V* data at room temperature, in atmosphere of nitrogen (■) and 90 ppm of acetone (●).

The author thanks Dr. E C Pereira (Department Chemistry, University Federal, Brazil) for the samples.

References

1. Wang, L X.; Li, X. G.; Yang, Y. L. Reactive Funct Polym 2001, 47, 125.
2. Bai, H.; Shi, G. Sensors 2007, 7, 267.
3. Han, D. H.; Lee, H. J.; Park, S. M. Electrochim Acta 2005, 50, 3085.
4. Khomenko, V.; Frackowiak, E.; Beguin, A. Electrochim Acta 2005, 50, 2499.
5. Johanson, U.; Marandi, A.; Tamn, T. Electrochim Acta 2005, 50, 1523.
6. Krivan, E.; Peintler, G.; Visy, C. Electrochim Acta 2005, 50, 1529.
7. Carquigny, S.; Sanchez, J. B.; Berger, F.; Lakard, B.; Lallemand, F. Talanta 2009, 78, 199.
8. Azioune, A.; Siroti, F.; Tanguy, J.; Jouini, M.; Chehimi, M. M.; Miksa, B.; Slomkowski, S. Electrochim Acta 2005, 50, 1661.

9. Saoudi, B.; Despas, C.; Chehimi, M. M.; Jammul, N.; Delamar, M.; Bessiere, J.; Walcarius, A. Sens Actuators B 2000, 62, 35.
10. Raoof, J. B.; Ojani, R.; Nadimi, S. R. Electrochim Acta 2004, 49, 271.
11. Hien, N. T. J.; Garcia, B.; Pailleret, C.; Deslouis, A. Electrochim Acta 2005, 50, 1747.
12. Partridge A.; Harris P. D. C.; Andrews, M. K. Analyst 1996, 12, 1349.
13. Kanazawa, K.; Diaz, A. F.; Geiss, W.; Gill, R. H.; Kwak, J. F.; Logan, J. A.; Rabolt, J. F.; Street, G. B. J Chem Soc Chem Commun 1979, 19, 854.
14. Lange, U.; Roznyatovskaya, N. V.; Mirsky, V. M. Analytica Chim Acta 2008, 164, 1.
15. Ram, M. K.; Yavuz O.; Aldissi, M. N. Synth Met 2005, 151, 77.
16. Geng, L.; Huang, X.; Zhao, Y.; Li, P.; Wang, S.; Zhang S.; Wu, S. H. Solid State Electron 2006, 50, 723.
17. Tai, H.; Jiang, Y.; Xie, G.; Yu, J.; Chen X.; Ying, Z. Sens Actuators B 2008, 129, 319.
18. Geng, L.; Zhao, Y.; Huang, X.; Wang, S.; Zhang S.; Wu, S. Sens Actuators B 2007, 120, 568.
19. Sakurai, Y.; Jung, H. S.; Shimanouchi, N.; Inoguchi, T.; Morita, S.; Kuboe, R. Natsukawa, K. Sens Actuators B 2002, 83, 270.
20. Likchodii, S. S.; Musa, K.; Cunnane, S. C. Clin Chem 2002, 48, 115.
21. Stranda, N.; Bhushana, A.; Schivob, M.; Kenyonb, N. J.; Davisa, C. E. Sens Actuators B 2010, 143, 516.
22. Cho, J. H.; Yu, J. B.; Kim, J. S.; Sohn, S. O.; Lee, D. D.; Huk, J. S. Sens Actuators B 2005, 108, 389.
23. Shen, Y.; Wan, M. J Polym Sci: Polym Chem 1997, 35, 3689.
24. Campos, M.; Simões, F. R.; Pereira, E. C. Sens Actuators B 2007, 125, 158.
25. Lee, J. Y.; Song, K. T.; Kim, S. Y.; Kim, J. C.; Kim, D. Y.; Kim, C. Y. Synth Met 1997, 84, 137.
26. Lee, C.; Lee, J. Y.; Lee, H. Synth Met 1997, 84, 149.
27. Scharz, K.; Pizzini, A.; Arendacka, B.; Zerlauth, K.; Filipiak, W.; Schmid, A.; Dizien, A.; Neuner, S.; Lechleitnu, S. S.; Burgi, W.; Miekisch, J.; Schubert, K.; Unterkofler, W.; Witkovsky, G.; Gastl, A.; Ammann, M. J Breath Res 2009, 3, 027003.
28. Chou, J. Hazardous Gas Monitors 1st edn., McGraw-Hill: New York, 2000.
29. Saxena, V.; Santhanam, K. S. V. Curr Appl Phys 2003, 3, 227.
30. Campos, M.; Cavalcante, E. M.; Kalinowski, J. J Polym Sci: Polym Phys 1996, 34, 623.
31. Rhoderick, E. H.; Williams, R. H. Metal Semiconductor Contacts, 2nd edn., Clarendon: Oxford, 1988.
32. Altindal, S.; Dökme, I.; Bülbül, M. M.; Yalçin, N.; Serin, T. Microelectronic Eng 2006, 83, 499.
33. Aydogan, S.; Saglam, M.; Türüt, A. Appl Surf Sci 2005, 250, 43.
34. Chand, S.; Bala, S. Physica B: Condensed Matter 2007, 390, 179.
35. Zeng, L.; Xia, Z.; Du, G.; Kang, J.; Han, R. O.; Liu, X. IEEE Trans Nanotechnol 2009, 8, 10.
36. Oh, J. W.; Lee, C.; Kim, N. J Chem Phys 2009, 130, 134909.
37. Akkiliç, K.; Türüt, A.; Çankaya, G.; Kiliçoglu, T. Solid State Commun 2003, 125, 551.
38. Tallman, D. E.; Vang, C.; Wallace, G. G.; Bierwagen, G. P. J Electrochem Soc 2002, 149, 173.
39. Ruangchay, L.; Schwank, J.; Sirivat, A. App Surf Sci 2002, 199, 128.
40. Ayyildiz, E.; Türüt, A.; Efeoglu, H.; Tüzemen, S.; Saglan. M.; Yogurtçu, Y. K. Solid State Electron 1996, 39, 83.
41. Wu, C. Y. J Appl Phys 1980, 51, 3786.
42. Cheung, S. K.; Cheung, N. W. Appl Phys Lett 1986, 49, 85.
43. Tataroglu, A.; Altindal, S. Microelectron Eng 2006, 83 2021.
44. Voigt, M.; Sokolowski, M. Mater Sci Eng B 2004, 109, 99.
45. Çetinkara, H. A.; Türüt, A.; Zengin, D. M.; Eirel, S. Appl Surf Sci 2003, 207, 190.